AD-A075 109 ARMY MISSILE COMMAND REDSTONE ARSENAL AL TECHNOLOGY LAB F/G 17/8
AUTOMATED LASER SPECKLE INTERFEROMETRY DISPLACEMENT CONTOUR ANA--ETC(U)
JUL 79 J A SCHAEFFEL
UNCLASSIFIED DRSMI-T-79-1 NL

1 OF 1
AD A075109

END
DATE FILMED
11-79
DDC

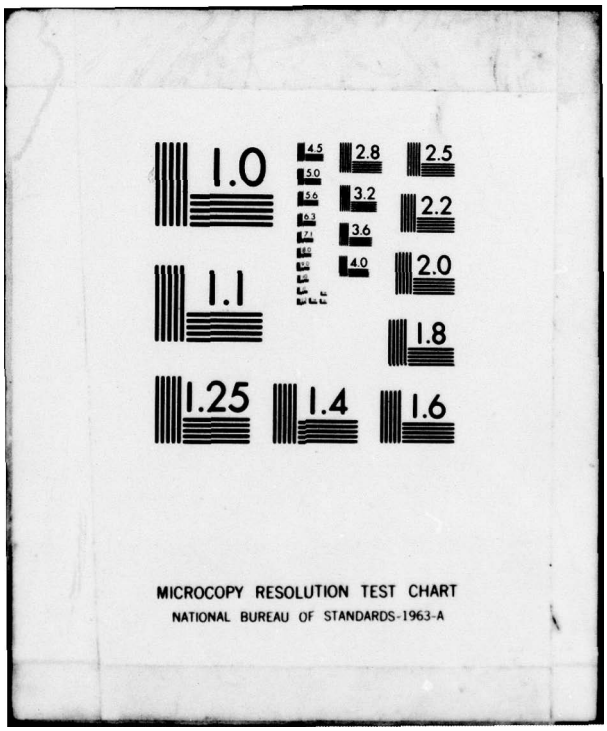
1.0
1.1
1.25
1.4
1.6
1.8
2.0
2.2
2.5
2.8
3.2
3.6
4.0
4.5
5.0
5.6
6.3
MICROCOPY RESOLUTION TEST CHART
NATIONAL BUREAU OF STANDARDS-1963-A

AD A075109

TECHNICAL REPORT T-79-71

LEVEL II

AUTOMATED LASER SPECKLE INTERFEROMETRY DISPLACEMENT CONTOUR ANALYZER

John A. Schaeffel, Jr.,
Technology Laboratory

2 July 1979

DDC
RECEIVED
OCT 17 1979
A

U.S. ARMY MISSILE COMMAND
Redstone Arsenal, Alabama 35809

DDC FILE COPY

Approved for public release; distribution unlimited.

SMI FORM 1021, 1 JUL 79 PREVIOUS EDITION IS OBSOLETE

79 10 17 040

DISPOSITION INSTRUCTIONS

DESTROY THIS REPORT WHEN IT IS NO LONGER NEEDED. DO NOT RETURN IT TO THE ORIGINATOR.

DISCLAIMER

THE FINDINGS IN THIS REPORT ARE NOT TO BE CONSTRUED AS AN OFFICIAL DEPARTMENT OF THE ARMY POSITION UNLESS SO DESIGNATED BY OTHER AUTHORIZED DOCUMENTS.

TRADE NAMES

USE OF TRADE NAMES OR MANUFACTURERS IN THIS REPORT DOES NOT CONSTITUTE AN OFFICIAL ENDORSEMENT OR APPROVAL OF THE USE OF SUCH COMMERCIAL HARDWARE OR SOFTWARE.

(14) DRSMI-T-79-1

UNCLASSIFIED
SECURITY CLASSIFICATION OF THIS PAGE (When Data Entered)

REPORT DOCUMENTATION PAGE	READ INSTRUCTIONS BEFORE COMPLETING FORM
1. REPORT NUMBER: T-79-71	2. GOVT ACCESSION NO. / 3. RECIPIENT'S CATALOG NUMBER
4. TITLE (and Subtitle): (6) Automated Laser Speckle Interferometry Displacement Contour Analyzer	5. TYPE OF REPORT & PERIOD COVERED: (9) Technical Report (12)
	6. PERFORMING ORG. REPORT NUMBER
7. AUTHOR(s): (10) John A. Schaeffel, Jr.	8. CONTRACT OR GRANT NUMBER(s): (12) 43
9. PERFORMING ORGANIZATION NAME AND ADDRESS: Commander, US Army Missile Command, ATTN: DRSMI-TL (R&D), Redstone Arsenal, Alabama 35809	10. PROGRAM ELEMENT, PROJECT, TASK AREA & WORK UNIT NUMBERS
11. CONTROLLING OFFICE NAME AND ADDRESS: Commander, US Army Missile Command, ATTN: DRSMI-TI (R&D), Redstone Arsenal, Alabama 35809 (11)	12. REPORT DATE: 2 July 1979 13. NUMBER OF PAGES: 42
14. MONITORING AGENCY NAME & ADDRESS (if different from Controlling Office)	15. SECURITY CLASS. (of this report): Unclassified 15a. DECLASSIFICATION/DOWNGRADING SCHEDULE

16. DISTRIBUTION STATEMENT (of this Report)
Approved for public release; distribution unlimited.

17. DISTRIBUTION STATEMENT (of the abstract entered in Block 20, if different from Report)

18. SUPPLEMENTARY NOTES

19. KEY WORDS (Continue on reverse side if necessary and identify by block number)

Speckle Interferometry
Displacement Analysis
Nondestructive Testing
Contour Mapping
Composite Material Testing
Young's Fringes
Computer Aided Fringe Analysis
Flaw Detection

20. ABSTRACT (Continue on reverse side if necessary and identify by block number)

This work presents a new technique and experimental equipment to analyze Young's Fringe speckle interferograms. A new method using an off-axis optical photodetector was developed for generating displacement contour maps of bodies when deformed under load. Laser speckle interferograms are made of the deformed body and analyzed with a special displacement contouring computer analyzer. Interferograms of a flawed composite tube were analyzed by the system and are presented in the work. Currently operating at about 20% of its maximum rated speed, the system can analyze 5000 data points in less than four minutes. This

→ next Page

DD FORM 1 JAN 73 1473 EDITION OF 1 NOV 65 IS OBSOLETE

UNCLASSIFIED
SECURITY CLASSIFICATION OF THIS PAGE (When Data Entered)

393 427

JOB

20. report presents both the theory and hardware which may be utilized to generate displacement contour maps of deformed bodies.

CONTENTS

Accession For
NTIS GRA&I
DDC TAB
Unannounced
Justification
By
Distribution/
Availability Codes
Dist | Avail and/or special

ILLUSTRATIONS

ILLUSTRATIONS

Figure Page

1. INTRODUCTION

The analysis of laser speckle interferograms is often a tedious and time consuming task. Many attempts have been made toward automating the analysis process with excellent success. The only major drawbacks have been in the time required and cost effectiveness of the process. With the idea of reducing cost, decreasing processing time and increasing reliability a new technique was sought for interpreting speckle interferograms. The new method utilizes an off-axis photosensor element coupled to a mini-computer to achieve these goals.

Laser speckle interferograms are most commonly used to make deformation measurements of deformable bodies.[1] *Figure 1* illustrates the basic method for making a laser speckle interferogram. When a diffuse surface of a structure is illuminated with coherent radiation, a grainy speckle effect is imaged by the eye or film plane of a camera due to the interference of light from the structure. This speckle effect is enhanced when the structure has microscopic surface irregularities. If the optical configuration remains fixed, the speckle pattern of the test object may be recorded on the film plane of a camera. Further, if the structure is deformed, the speckle points shift with the deformation and a second exposure of the deformed speckle pattern can be made.

Using a technique of double exposure, speckle interferograms of a structure are normally made by photographing the speckle pattern in a deformed and undeformed configuration. A beam of laser light is then passed through a region of the double exposure where the local deformation is desired. As the beam passes through the film, the deformed and undeformed speckle recorded there diffract the laser light and cause an interference effect on a viewing screen. A diffraction halo modulated by light and dark bars of light is produced where the distance 2d between bars is inversely proportional to the distance between the undeformed and deformed speckle on the film plane. A normal to the light and dark bar pattern indicates the axis of deformation of the speckle. The theory to be developed assumes that the deformation region illuminated by the laser beam in reconstruction is uniform and that the linear optical theory is applicable.[2]

Although the laser speckle interferograms can be made rather quickly, the analysis time of a single illuminated point can be very significant, i.e., several seconds. When a full field analysis is required, the time limitation can be severe if several thousand points of deformation data are

1. J.A. Schaeffel, *Acoustical Speckle Interferometry*, US Army Missile Research and Development Command, Redstone Arsenal, Alabama, Technical Report T-79-39, 22 March 1979.
2. J.A. Schaeffel, B.R. Mullinix, W.F. Ranson, and W.F. Swinson, *Computer Aided Optical Nondestructive Flaw Detection System for Composite Materials*, US Army Missile Research and Development Command, Redstone Arsenal, Alabama, Technical Report T-78-5, 26 September 1977.

PRECEDING PAGE NOT FILMED
BLANK

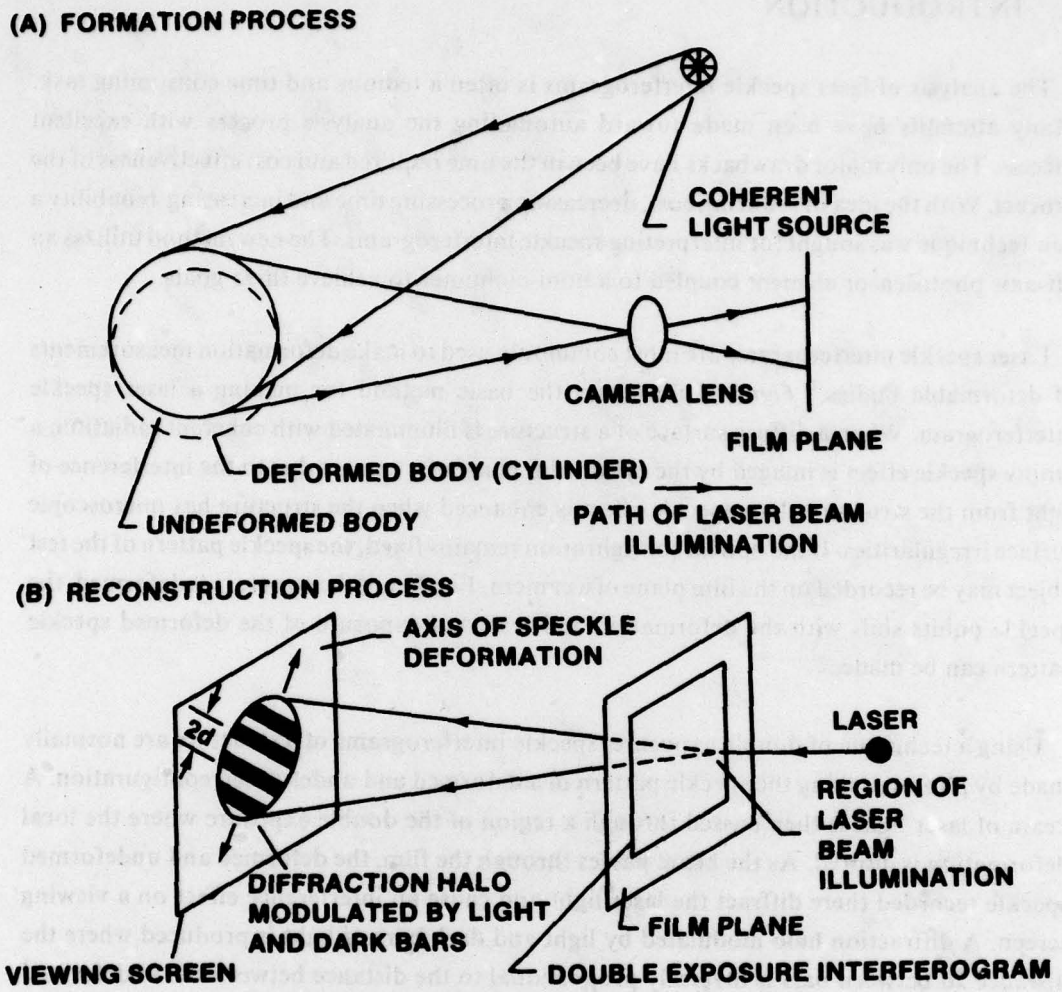

Figure 1. Laser speckle interferometry configuration.

needed. Therefore, a rapid low-cost device is needed which can generate contours of constant displacement over a full-field interferogram.

2. THEORETICAL DEVELOPMENT

Figure 2 illustrates the reconstructed diffraction halo modulated by light and dark bars of light. From the linear theory,[2] the displacement in the θ direction of a point on the body is given as:

$$u_\theta = \frac{S\lambda f}{2d} \tag{1}$$

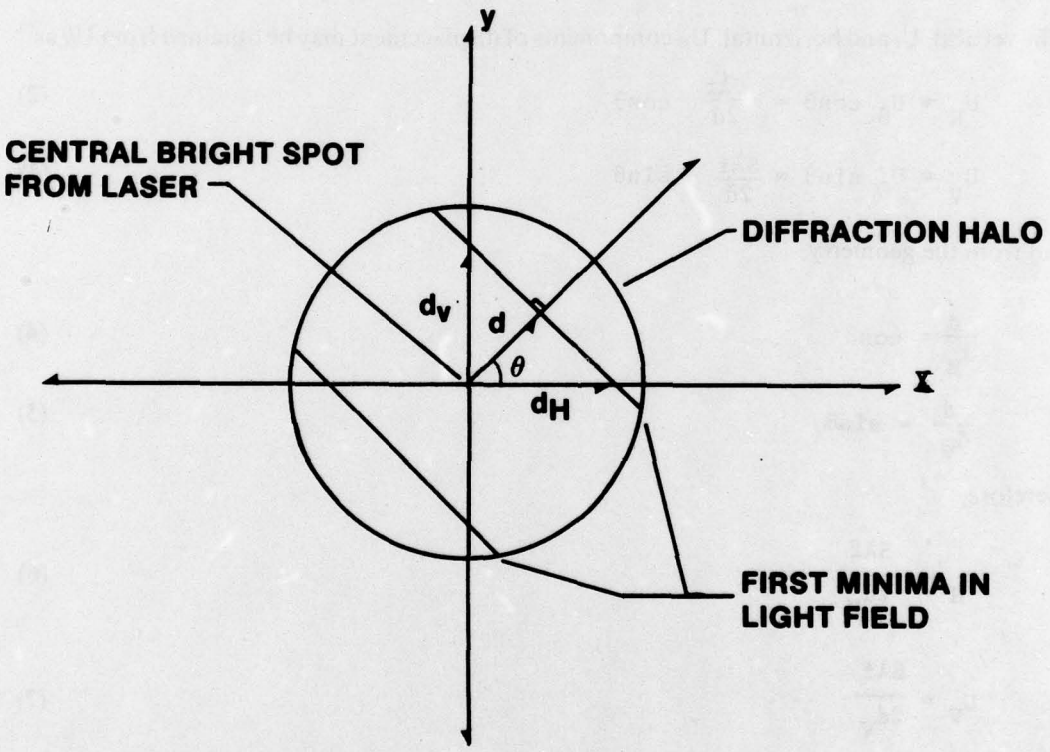

Figure 2. Diffraction halo geometry.

where,

S ≡ film scale factor (magnification ratio).

λ ≡ wavelength of laser illumination source.

f ≡ distance from interferogram to analyzer screen.

d ≡ distance from central bright spot to first minima.

U_θ ≡ displacement of the point illuminated by the laser on the object in the θ direction.

The vertical, U_V and horizontal, U_H components of displacement may be obtained from $U\theta$ as:[3]

$$U_H = U_\theta \cos\theta = \frac{S\lambda f}{2d} \cos\theta \quad (2)$$

$$U_V = U_\theta \sin\theta = \frac{S\lambda f}{2d} \sin\theta \quad (3)$$

and from the geometry,

$$\frac{d}{d_H} = \cos\theta \quad (4)$$

$$\frac{d}{d_V} = \sin\theta \quad (5)$$

therefore,

$$U_H = \frac{S\lambda f}{2d_H} \quad (6)$$

$$U_V = \frac{S\lambda f}{2d_V} \quad (7)$$

The optical configuration of *Figure 3* shows a photodetector placed off-axis a distance *X* from the laser central bright spot and in the field of the diffraction halo. The photodetector senses the light intensity. Whenever a minima in intensity is detected, the fringe order at the illumination point is an integral number n = 1, 2, 3, ... in value.

3. J.A. Schaeffel, *Lab Notebook 7232*, US Army Missile Research and Development Command, Redstone Arsenal, Alabama, 10 November 1978.

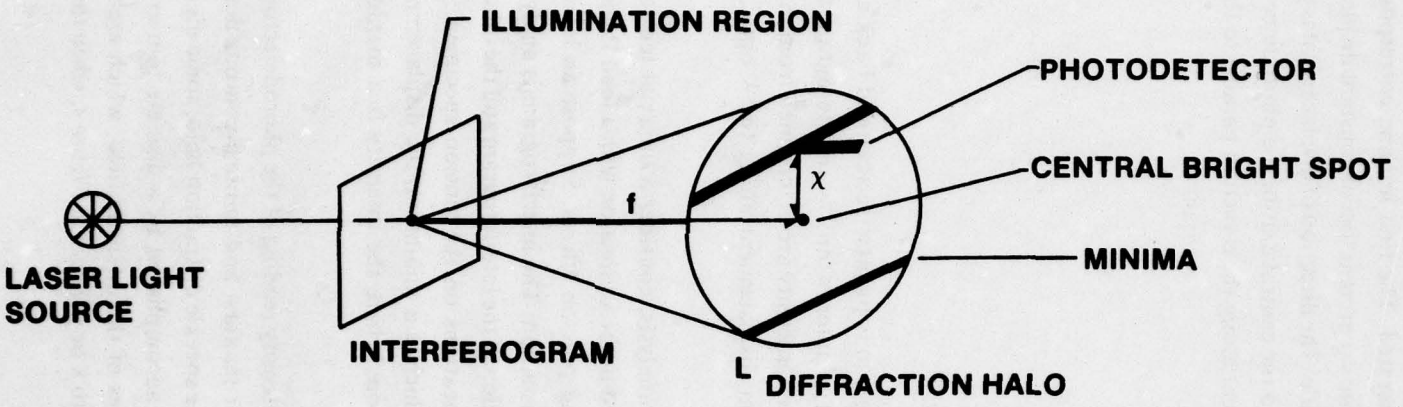

Figure 3. Photodetector optical geometry.

By moving the interferogram in a raster fashion and recording the intensity at each point, contours of constant n are generated. The first minima corresponds to n = 1, the second minima n = 2, etc. These contours represent loci of constant displacement on the body from which the interferogram was made. The direction of displacement is parallel to the axis formed from the central bright spot and the central axis of the photodetector. Once n is known at a particular point, the displacement along the direction parallel to the X axis is given as:

$$U_X = n\left\{\frac{S\lambda f}{2X}\right\} = n\nu \tag{8}$$

where,

$$\nu = \frac{S\lambda f}{2X} \tag{9}$$

an optical geometrical constant.

In operation the interferogram is pointwise scanned back and forth in front of the photodetector. For each point of interest on the interferogram the intensity is recorded. Contours of minima and maxima intensity are determined from this record. These contours correspond to lines of constant displacement along the X optical axis as determined by Equation 8.

To illustrate the method of analysis, consider a uniaxial tension specimen as shown in *Figure 4*. The specimen is loaded in the x direction with a load P which causes a deformation parallel to the x axis neglecting poisson effects. Suppose an interferogram is made of the structure before and after deformation. The interferogram is analyzed with a photodetector offset a distance X in the x direction of the interferogram and the intensity is shown plotted as a function of x and Y for 24 locations on the tension specimen. At each location on the interferogram intensity plot which is a minimum, the displacement is an integral number n = 0, 1, 2, ... of ν. At locations where the intensity is a maximum the displacement is n = 1/2, 3/2, 5/2, ... of ν.

In a practical situation the intensity reading of the photodetector is digitized and stored in digital form by a computer for maxima and minima contour determinations. Due to the inherent noise found in the laser speckle diffraction halo, some digital filtering of the optical signal is desired. This may be accomplished by a discrete fourier transform (DFT) of the intensity field. Given N samples of the intensity field, which are uniformly separated and collinear along an axis parallel to x or y, shown in *Figure 4*, when the frequency domain of the transformed field is given as:[4]

4. J.A. Betts, *Signal Processing Modulation and Noise*, American Elsevier Publishing Company, Inc., New York, 1971.

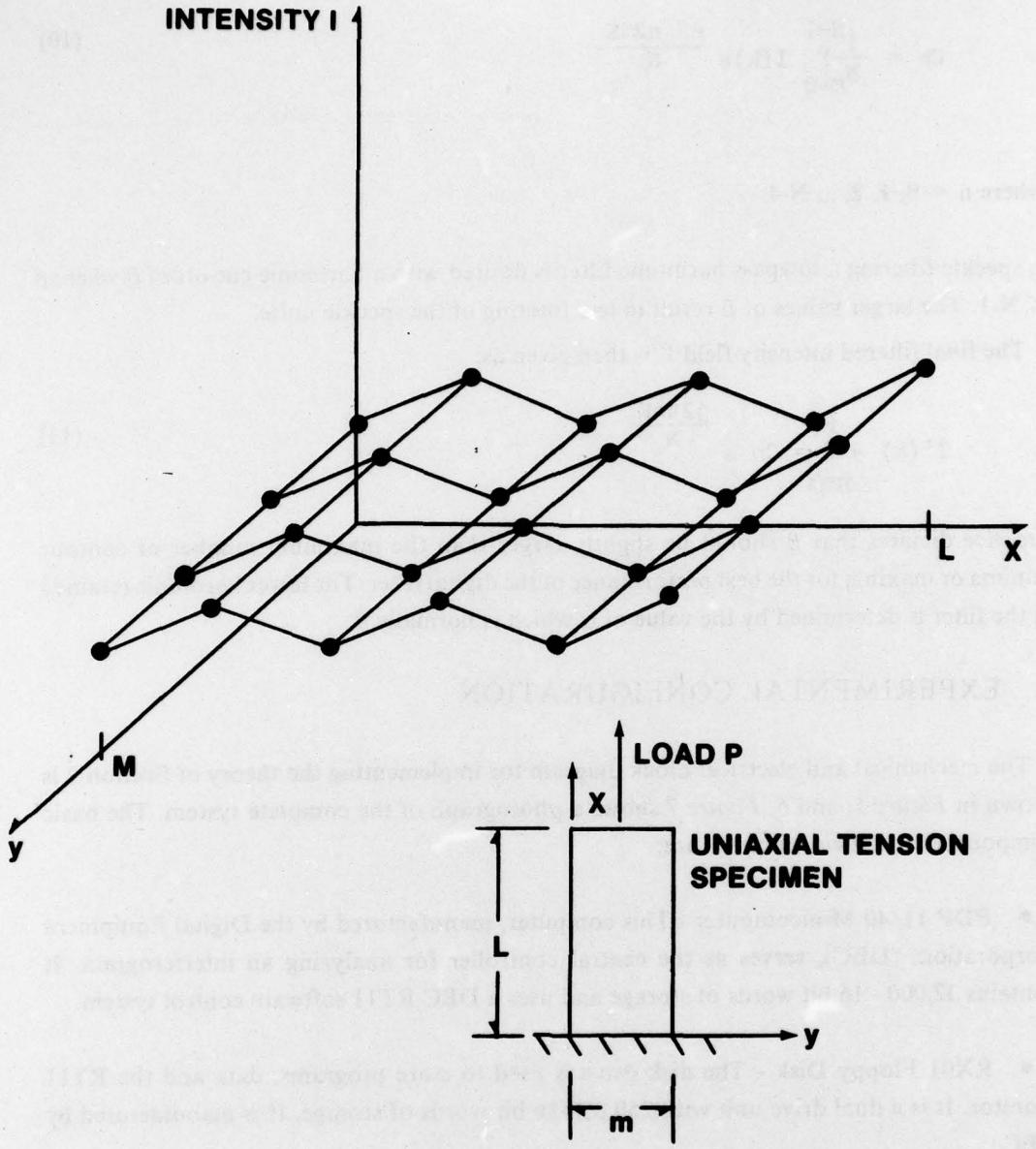

Figure 4. Intensity plane configuration for uniaxial test specimen.

$$Cn = \frac{1}{N}\sum_{K=0}^{N-1} I(k)\, e^{\frac{-J\, n2\pi K}{N}} \qquad (10)$$

where n = 0, 1, 2, ... N-1 .

In speckle filtering a lowpass harmonic filter is desired with a harmonic cut-off of β where $\beta < N-1$. The larger values of β result in less filtering of the speckle noise.

The final filtered intensity field I′ is then given as:

$$I'(k) = \sum_{n=\alpha}^{\beta} Cn\, e^{\frac{j2\pi nK}{N}} \qquad (11)$$

Practice dictates that β should be slightly larger than the maximum number of contour minima or maxima for the best performance of the digital filter. The lower harmonic retained in the filter is determined by the value of α which is normally 0.

3. EXPERIMENTAL CONFIGURATION

The mechanical and electrical block diagram for implementing the theory of Section 2 is shown in *Figure 5*, and *6*. *Figure 7* shows a photograph of the complete system. The basic components and their functions are:

- PDP 11/40 Minicomputer - This computer, manufactured by the Digital Equipment Corporation, (DEC), serves as the central controller for analyzing an interferogram. It contains 32,000 - 16 bit words of storage and uses a DEC RT11 software control system.

- RX01 Floppy Disk - The disk drive is used to store programs, data and the RT11 monitor. It is a dual drive unit with 250,000-16 bit words of storage. It is manufactured by DEC.

- DECWRITER - This is the typewriter input-output port for the computer. It is a 30 character per second unit used to input scan parameters for analyzing an interferogram and printing the results of the scanning process. It is manufactured by DEC.

- AR11 - This unit is the analog input port manufactured by DEC. It is used to digitize the photodetector intensity signal. The unit features a 16-channel A/D converter with an input

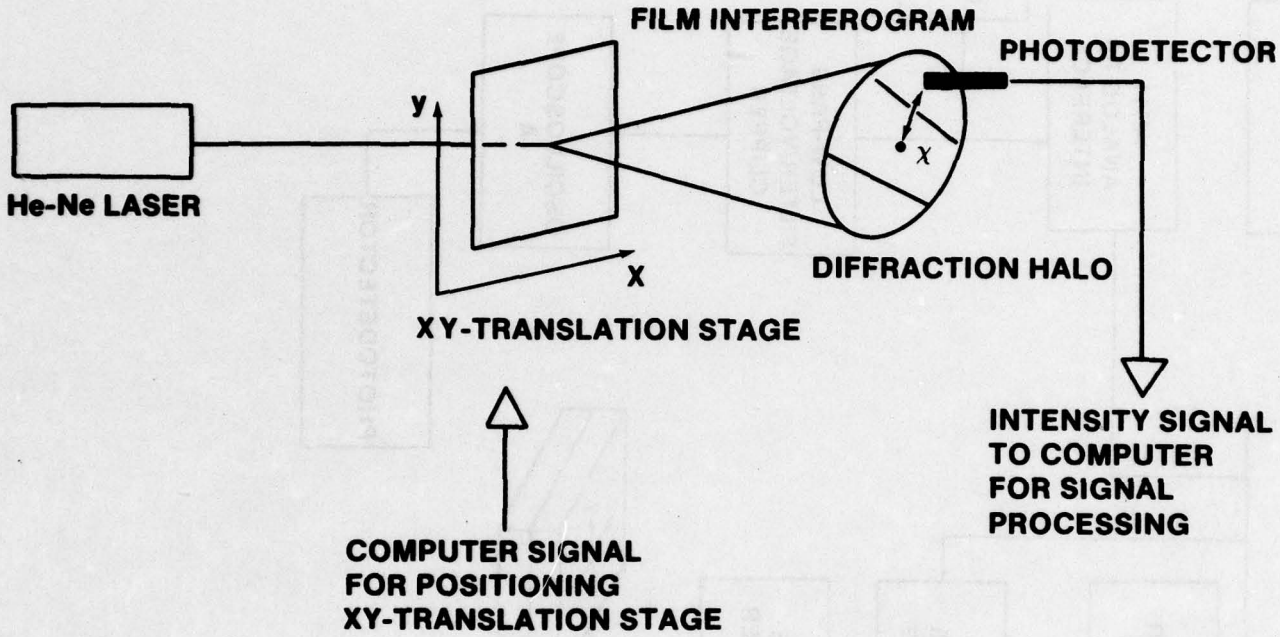

Figure 5. Experimental mechanical configuration.

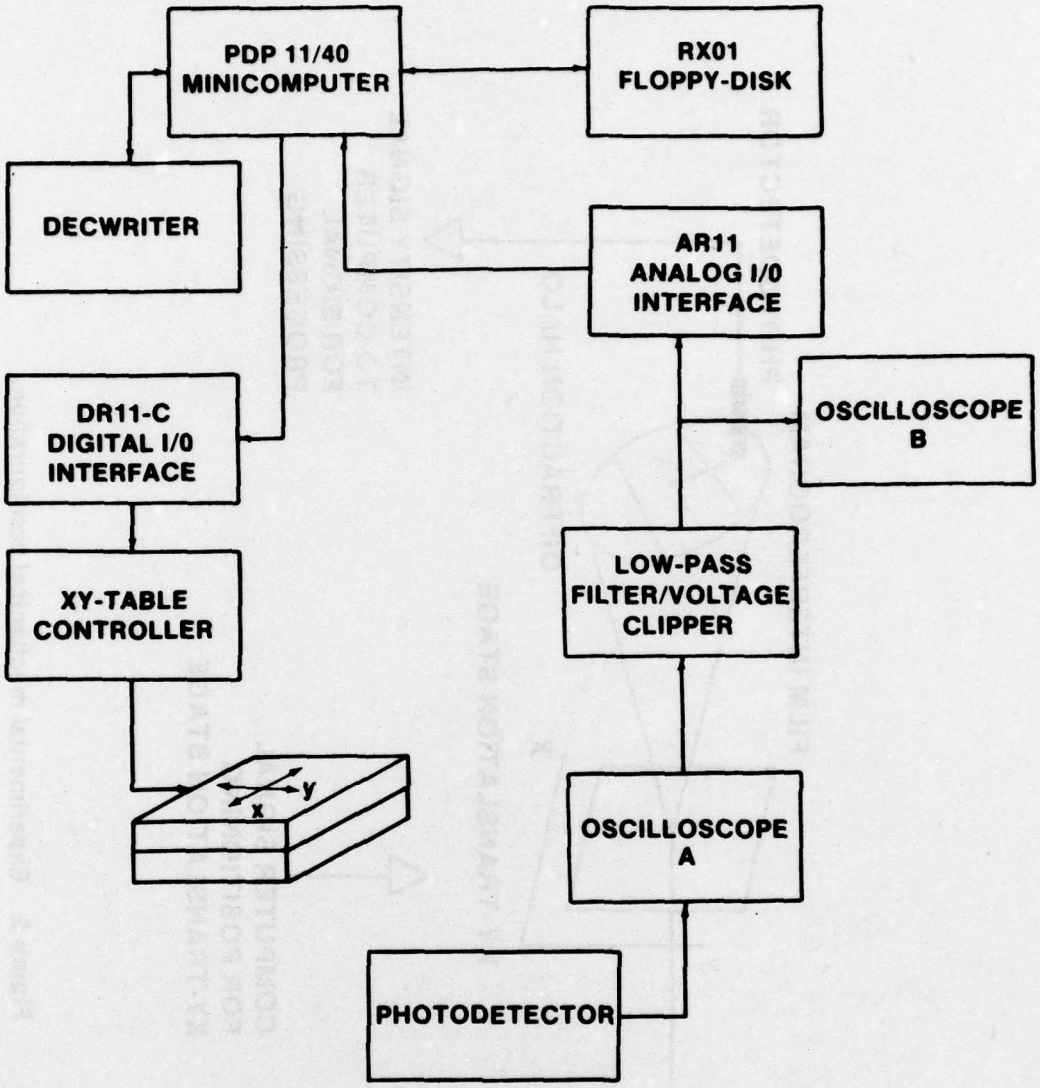

Figure 6. Experimental electrical configuration.

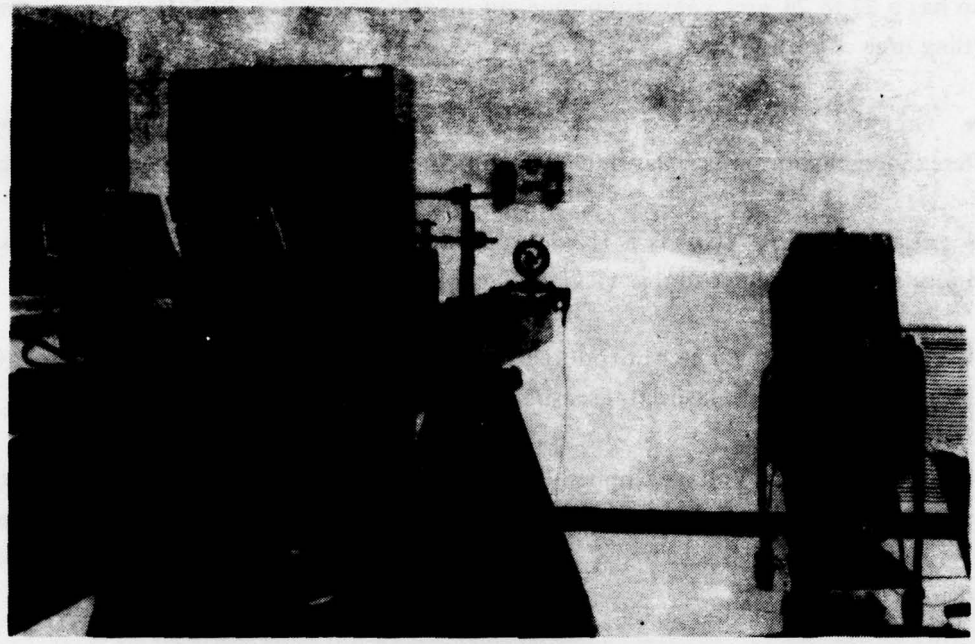

Figure 7 (a). Optical Bench Configuration.

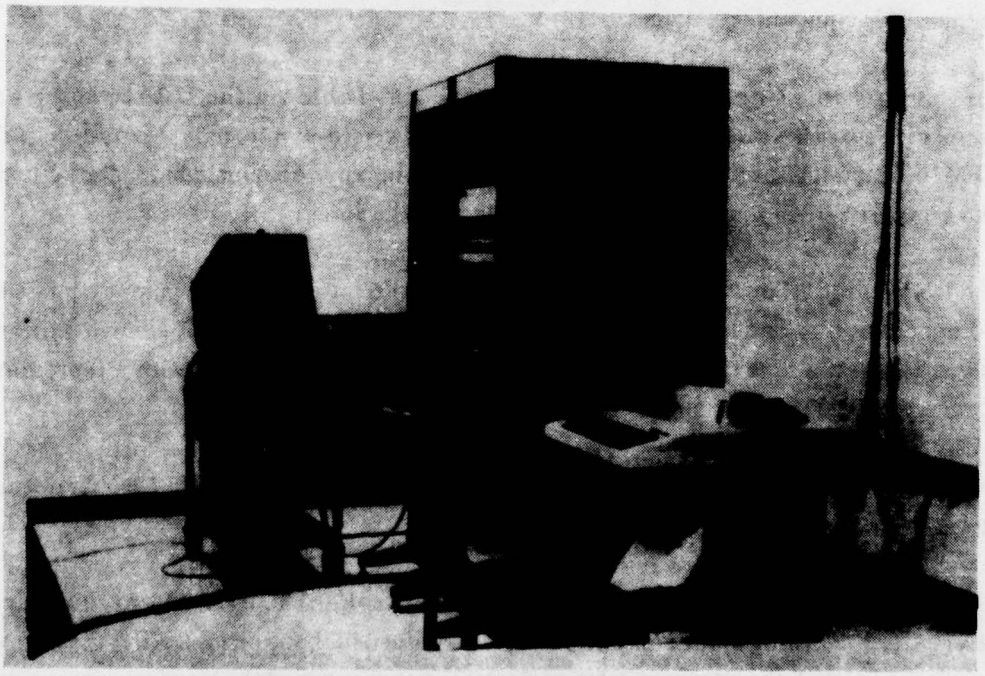

Figure 7 (b). Computer System.

voltage range of 0 to + 5 V, a resolution of 10 bits, and an accuracy of ±0.1% of full scale. It also has a 22 to 24 μsec conversion time, an input impedance of 10 MΩ and a maximum settling time of 8μsec.

- Oscilloscope A - This is a Tektronix Company Model 549 oscilloscope with a type W differential comparator used as a high gain amplifier to amplify the photodetector signal.

- Oscilloscope B - This is a Hewlett-Packard Model HP1700B oscilloscope used to monitor the input voltage to the AR11 A/D converter.

- Photodetector - The photodetector selected is a Spectra Physics Model 401C photodetector with a peak spectral sensitivity at 6328 angstroms.

- LowPass Filter/Voltage Clipper - This circuit consists of a lowpass frequency passive filter and voltage clipper. The RC time constant is 0.1445 ΩF with a cut-off clip voltage of about 3.8 V. The circuit is used to reduce signal noise and prevent a voltage overload condition to the AR11.

- DR11C-The DR11C is a digital I/0 interface used to position xY-table for scanning interferograms. It is manufactured by DEC and features 16 ports of input and 16 ports of output TTL compatible voltages.

- XY - Table Controllers - Control of the XY-Table via the DR11C interface is maintained by these units. This system contains two slo-syn translator modules (Type STM101) manufactured by the Superior Electric Company. Also included in the system are two type MPS-1000 power supplies also made by Superior.

- XY-table - The XY-table used to position the interferogram is made by Design Components, Inc., and is a Model DC-66 having a scanning range of 152.4 mm in the x and Y directions. It can take single steps between scan points of 0.0254 mm with a repositioning accuracy of 0.00254 mm.

- He-Ne laser - The laser selected was a Spectra-Physics Model 124 He-Ne laser operating at 6328 Å.

Operation of the optical system is controlled through the PDP 11/40 computer. A description and listing of the computer code is contained in the appendix. After the computer program is started, the parameters for performing a raster scan of the interferogram are input

to the computer through the DECWRITER. A total of 100 points in the x direction and 50 points in the y direction may be scanned for a total of 5000 points. After the scanning parameters are input to the computer, a request is made for the initial position for scanning. The operator then positions the interferogram interactively with the computer. Once this operation is complete the interferogram is scanned by moving it to each scan point automatically and the photodetector intensity signal is digitized by the computer. This entire operation is automatic. If, during the scanning process, the operator needs to stop scanning and return to the initial scan position, the setting of any bit on the control console may perform this function. After the scan is made, a DFT filter operation is performed if requested, and a contour plot of the results is made. While the contour plot is being made, the results can be modified by selecting the proper bit configuration on the computer console. A listing of these commands is contained in the appendix.

The method of contour plotting selected involves the use of a variable reference signal intensity plane. Intensity information from the photodetector is stored as a digital signal floating point level from 0.0 to 1.0 in the computer memory and may be represented in graphical form as in *Figure 4*. To make a contour plot of deformation, the operator specifies a signal ratio from 0.0 to 1.0. All intensities stored in memory greater than the signal ratio are plotted as light regions (maxima) and all intensities less than the signal ratio are plotted as dark regions.

Smoothing of the contours is possible using the DFT filters provided. The filter may precede or follow after a contour plot is made.

4. EXPERIMENTAL RESULTS

In order to test the operation of the system and new scanning technique, a composite E-glass tube was fabricated using an Epon 828 resin system. *Figure 8* shows a schematic of the tube. Pertinent tube data includes the following:

- Cylinder No. 8-E-45-A
- Test Pressures 0-150 psig
- Cut Fiber Flaw
- E-glass, Epon 828 resin system
- 74.11 mm inside diameter
- 1.27 mm wall thickness
- 76.65 mm outside diameter
- 75.38 mm mean diameter

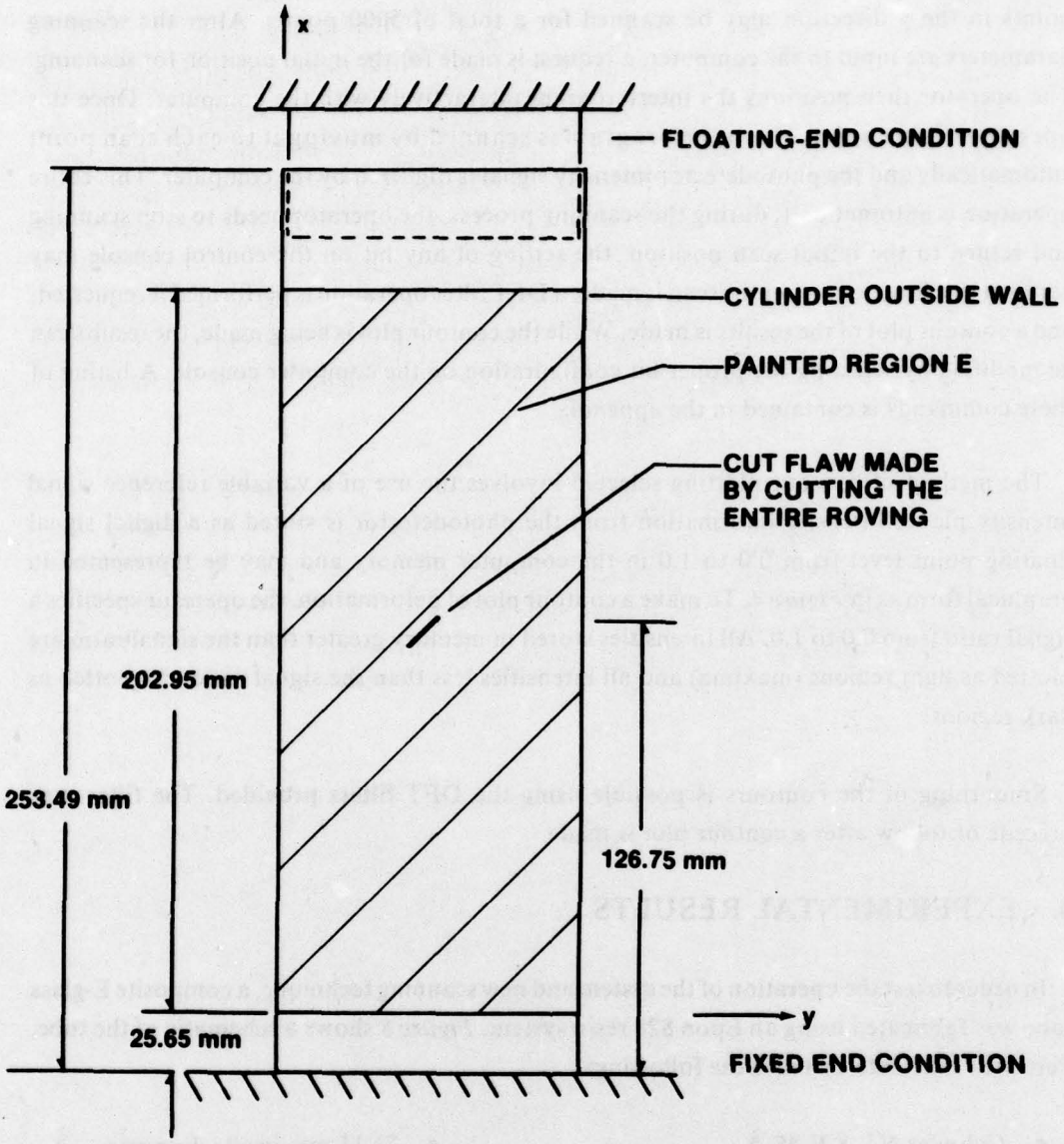

Figure 8. · Schematic of tube test specimen.

The tube had an overall length of 253.49 mm with a cut-flaw in the fiber 126.75 mm from the bottom of the tube. The tube was painted in the region marked E for a total of 202.95 mm. Specimen pressure testing was at 0 and 150 psig. Boundary conditions on the endcaps included a fixed-end condition at the base and a free-floating-end condition at the top of the tube. After pressurizing the tube to 150 psig, a laser photograph was made in the deformed condition and then the pressure was released. A second laser photograph was then made for the double exposure.

Analysis was done with a total of 100 points in the x direction and 50 points in the Y direction. The raster scan included a total of 5000 points. For the scanning process $X = 152.4$ mm, f=255.27 cm and ν=0.01209 mm/fringe order. The interferogram scanning increments in x and y covered the entire painted region uniformly. Inteferograms of the specimen were analyzed for the front and back surfaces with and without a flaw, respectively.

Figures 9 and *10* are contour displacement plots of the flawed cylinder surface made with the scanning system. Maxima are indicated with a (-) and minima with an (*). The horizontal row of numbers indicates the x axis scan position and the vertical column indicates the y axis scan position. The flawed region of the tube is indicated by a broad minima at location column 60, row 25. *Figures 11* and *12* indicate the results after using a DFT Filter. The filter parameters are $\alpha = 0$ and $\beta = 14$ in both x and y directions. As seen in *Figures 11* and *12*, there is a significant perturbation in the displacement contour map at the same location as in *Figures 9* and *10*. The results of the filter are to reduce the overall signal noise level. The difference in displacement between a maxima and a minima contour is 0.00605 mm. Therefore, high strain gradients are present in the tube at those locations where displacement contours have sharp changes in the x or y directions.

A series of scans followed by manual fringe digitizations were made and the results compared. In general, the percentage of difference between the automated and manual analysis differed by less than 4% for fringe orders of approximately $n \approx 1$. As n approaches values of 4 to 5 the measured displacements differ by less than 2%. The system is very fast and has a potential digitization rate of 6250 data points/min. Under certain optimum conditions 10^6 data points may be digitized in about 2 min if the distances between scan points is minimized.

An interesting test was made by plotting on an oscilloscope the intensity map as digitized by the computer and without filtering. *Figure 13* shows the result which may be compared with *Figures 9* and *10*. In this test, a composite tube with a similar flaw as before was analyzed and discontinuities in the fringe pattern can be observed.

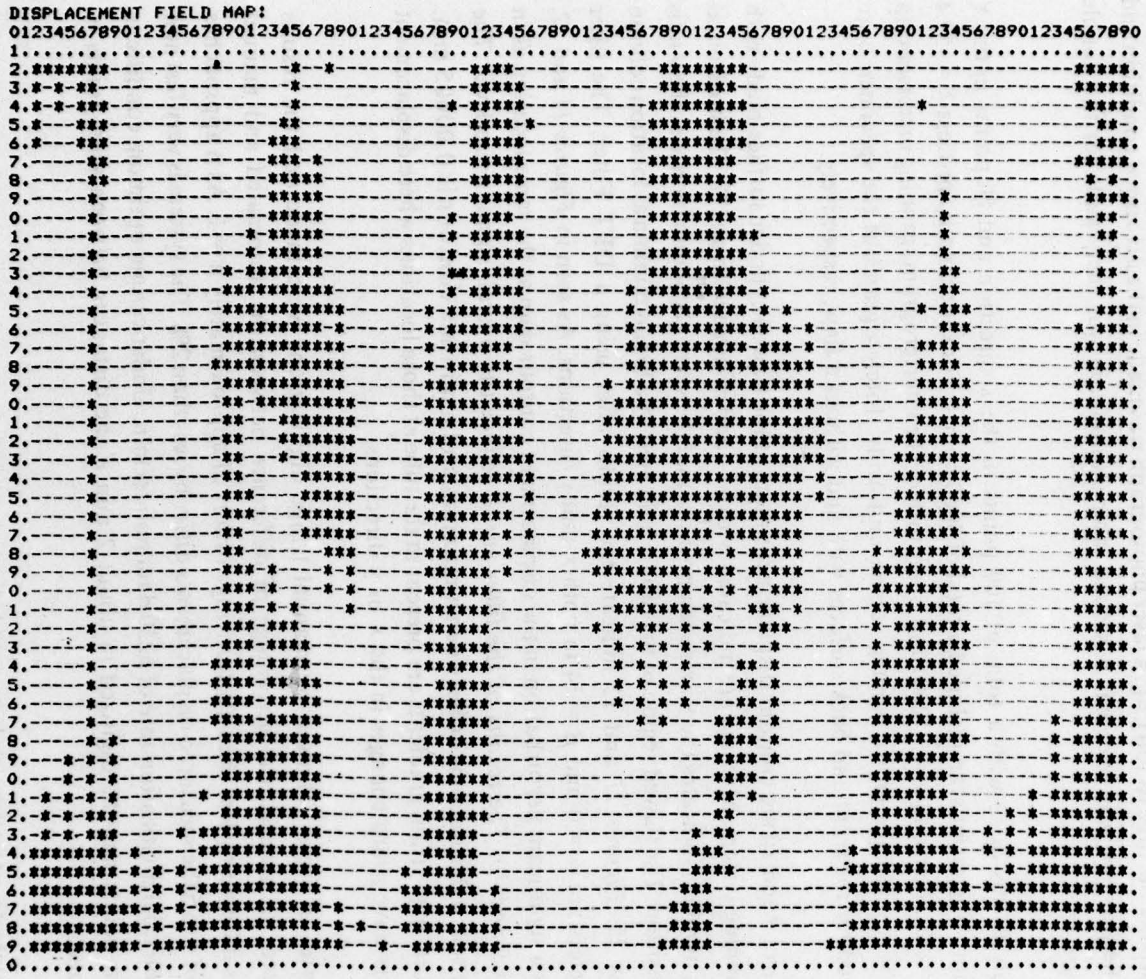

Figure 9. Flawed cylinder displacement contour map without discrete Fourier Transform Filter (front view). Signal ratio = 0.5.

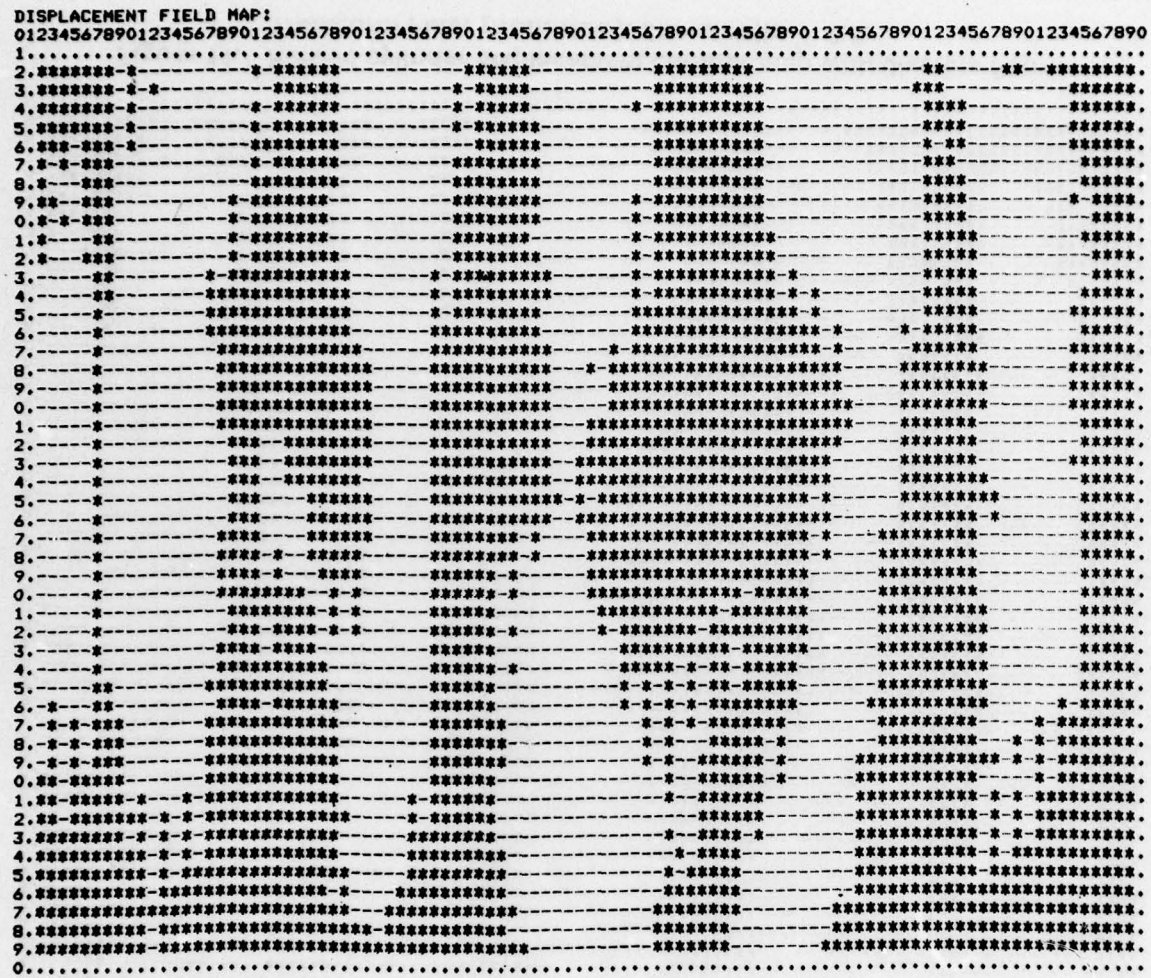

Figure 10. Flawed cylinder displacement contour map without discrete Fourier Transform Filter (front view). Signal ratio = 0.6.

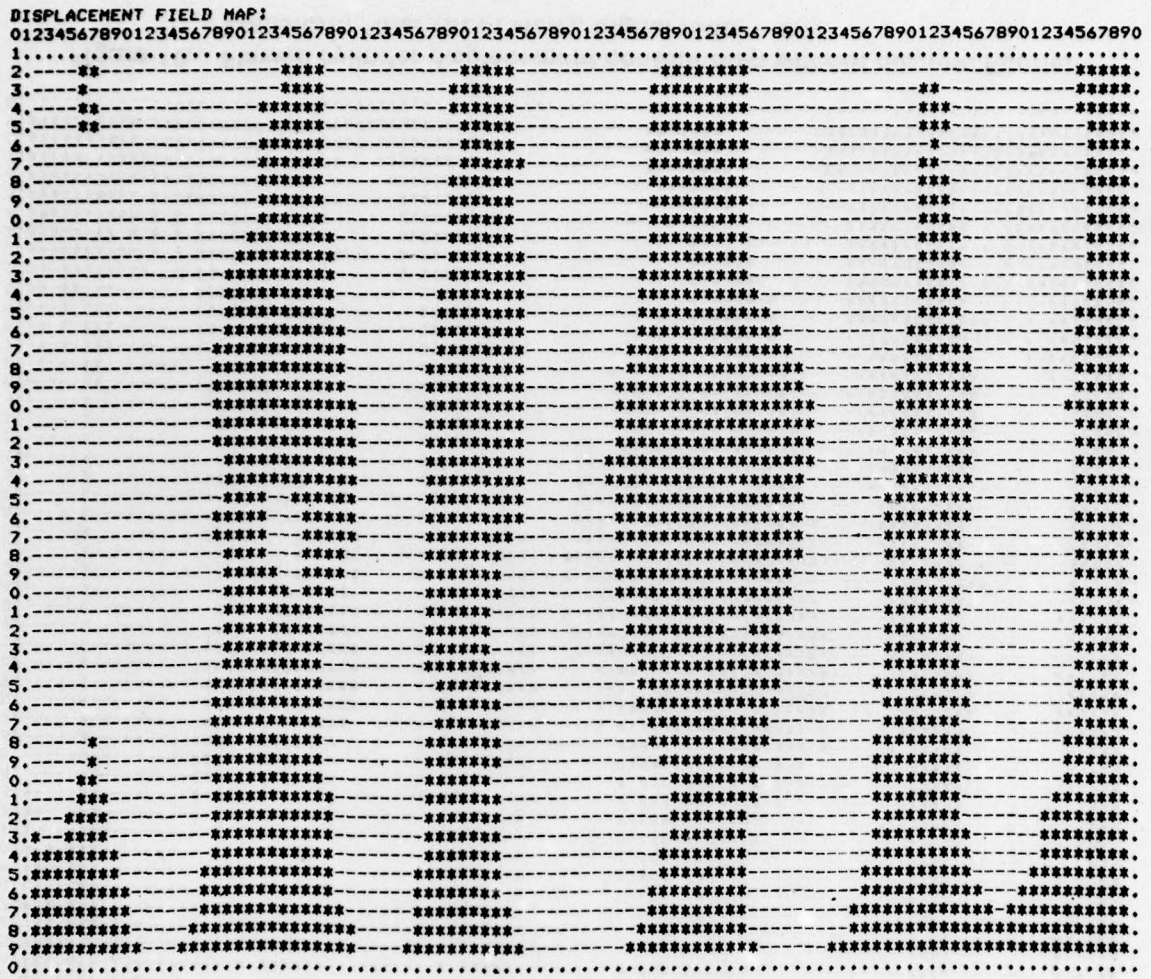

Figure 11. Flawed cylinder displacement contour map with discrete Fourier Transform Filter (front view). Signal ratio = 0.5.

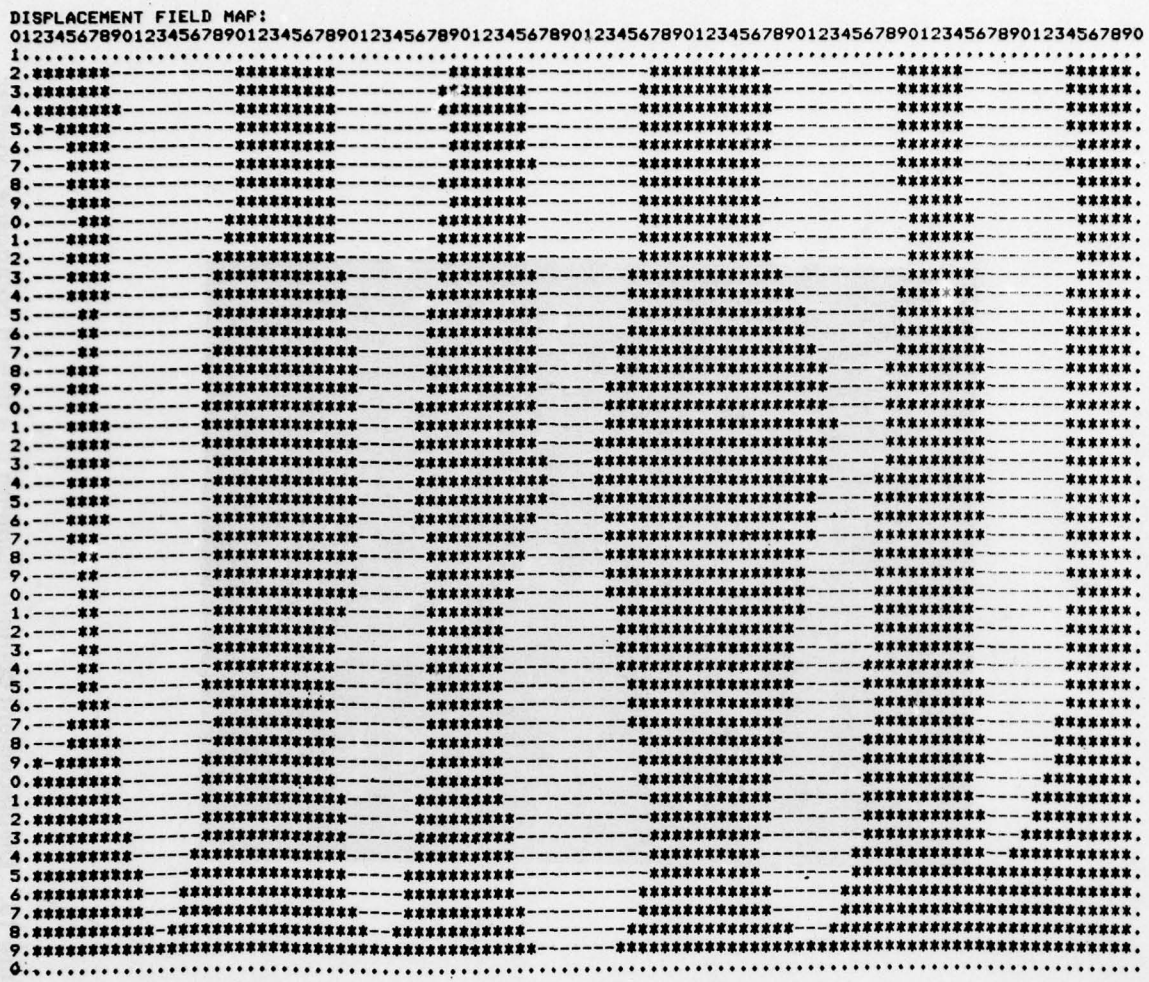

Figure 12. Flawed cylinder displacement contour map with discrete Fourier Transform Filter (front view). Signal ratio = 0.6.

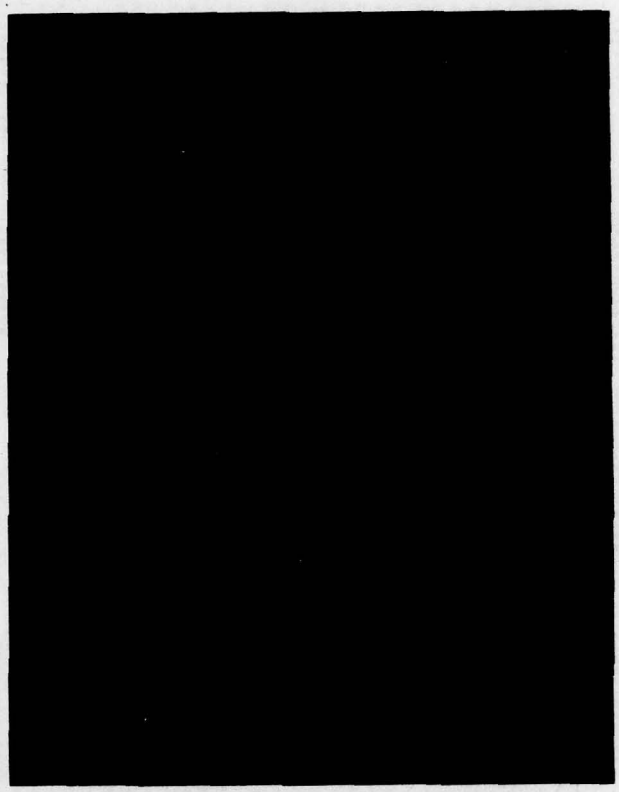

Figure 13. Displacement contour mapping of a flawed composite cylinder.

5. CONCLUSIONS

The theory and an experimental configuration were developed for automated displacement contour analysis of laser speckle interferograms. The number of displacement contours available is proportional to the number of diffraction fringe orders n available throughout the offset distance X. The system was checked to determine how well fringe contours could be measured and found to be accurate to at least 4% of the measured distance by hand. System scanning speed is extremely important, and it was found that 5000 data points could be analyzed in about 4 min when the system was operating at about 20% of its maximum rated speed. This is very encouraging for systems in which as many as 10^6 data points would be analyzed. Advantages of the present system over those of the past include virtual operator-free scanning, high speed, low cost and full field displacement field mapping.

APPENDIX

COMPUTER INPUT VARIABLES

PRECEDING PAGE NOT FILMED
BLANK

1. CONSOLE CONTROL SWITCHES (PDP 11/40):

Bit 0 = A new signal ratio will be requested for making a new contour plot immediately if this switch is turned on while a contour plot is being made.

Bit 1 = A new signal ratio will be requested for making a new contour plot at the end of the current contour plot if this switch is turned on.

Bit 2 = A new Discrete Fourier Transform filter parameter for filtering the current intensity signal will be requested at the end of the current contour plot if this switch is turned on.

Bit 3 = If turned on while contour plotting, a new set of scan parameters will be requested at the end of the current contour plot.

Bit 4 = If turned on while contour plotting, a set of new ASCII code plot symbols will be requested at the end of the current contour plot.

Bit 5 = If turned on, fringe orders may be ordered to displacement contours at the end of the current contour plot.

Bit 6 = End the program if turned on while contour plotting. The current contour plot is completed.

2. CODE VARIABLES:

IXP = total number of points in the x direction to be scanned.

IXS = number of 0.0254 mm increments between scan points in the x direction.

IYP = total number of points in the y direction to be scanned.

IYS = number of 0.0254 mm increments between scan points in the y direction.

IXF1 = α+1 for the x direction.

IXF2 = β+1 for the x direction.

PRECEDING PAGE NOT FILMED
BLANK

IYF1 = α+1 for the y direction.

IYF2 = β+1 for the y direction.

SR = signal ratio.

I1 = number of 0.0254 mm increments to advance the x stage before scanning.

I2 = number of 0.0254 mm increments to advance the y stage before scanning.

```
C-----PROGRAM SDFT
C-----WRITTEN BY: JOHN A. SCHAEFFEL, JR.
C-----BIT 0=NEW SR AT END OF PRINT LINE
C-----BIT 1=NEW SR AT END OF CONTOUR PLOT
C-----BIT 2=NEW DFT AT END OF CONTOUR PLOT
C-----BIT 3=NEW SCAN PARAMETERS
C-----BIT 4=NEW ASCII PLOT CODES
C-----BIT 5=EXAMINE FRINGES
C-----BIT 6=END PROGRAM
C-----ALL BITS MUST BE OFF FOR SCAN
C-----0-5 VOLTS AR11 RANGE
C-----INPUT STREAM ON AR11=3
      DIMENSION A(100,50),B(2,100),IT(101)
      KA1=72
      KA2=76
      WRITE(5,1)
1     FORMAT(' SDFT ANALYZER CODE')
41    WRITE(5,2)
2     FORMAT(' NO. X POINTS, X-SCAN INTERVAL-2I3')
      READ(5,3) IXP,IXS
3     FORMAT(2I3)
      WRITE(5,4)
4     FORMAT(' NO. Y POINTS, Y-SCAN INTERVAL-2I3')
      READ(5,3) IYP,IYS
      WRITE(5,11)
11    FORMAT(' DFT X,Y MIN-MAX FILTER LEVELS-4I3')
      READ(5,12) IXF1,IXF2,IYF1,IYF2
12    FORMAT(4I3)
      WRITE(5,13)
13    FORMAT(' SIGNAL RATIO-F10.0')
      READ(5,14) SR
14    FORMAT(F10.0)
10    WRITE(5,36)
36    FORMAT(' X,Y STAGE POSITION-2I4')
      READ(5,37) I1,I2
37    FORMAT(2I4)
      IF(I1.EQ.0.AND.I2.EQ.0) GOTO 38
      CALL XADV(I1,5)
      CALL YADV(I2,5)
      GOTO 10
38    CONTINUE
      IM=0
      IY1=1
      IY2=IYP
      IY3=1
      IXS=IABS(IXS)
      IYS=IABS(IYS)
      DO 6 I=1,IXP,1
      DO 5 J=IY1,IY2,IY3
      CALL IPOKE('170400,'21001)
      ITP=IPEEK('170402)
      A(I,J)=FLOAT(ITP)/1024.
      ITEST=IPEEK('177570)
      IF(ITEST.NE.0) GOTO 41
      IF(J.NE.IY2) CALL YADV(IYS,5)
5     CONTINUE
      IY4=IY1
      IY1=IY2
      IY2=IY4
      IY3=-IY3
      IYS=-IYS
      CALL XADV(IXS,5)
6     CONTINUE
      IXS=-IXS
```

```
      DO 7 I=1,IXP,1
      CALL XADV(IXS,5)
7     CONTINUE
      IF(IYS.GT.0) GOTO 9
      DO 8 J=1,IYP-1,1
      CALL YADV(IYS,5)
8     CONTINUE
9     CONTINUE
      IF(IXF1.EQ.0) GOTO 39
      IM=0
      C=6.283185
      D=FLOAT(IXP)
      DO 17 J=1,IYP,1
      DO 15 I=1,IXP,1
      B(1,I)=0.
15    B(2,I)=0.
      DO 16 K=IXF1-1,IXF2-1,1
      DO 16 L=0,IXP-1,1
      B(1,K+1)=B(1,K+1)+(A(L+1,J)*COS(FLOAT(K*L)*C/D))/D
      B(2,K+1)=B(2,K+1)-(A(L+1,J)*SIN(FLOAT(K*L)*C/D))/D
16    CONTINUE
      DO 17 M=0,IXP-1,1
      A(M+1,J)=0.
      DO 17 N=IXF1-1,IXF2-1,1
      A(M+1,J)=A(M+1,J)+B(1,N+1)*COS(FLOAT(N*M)*C/D)
      A(M+1,J)=A(M+1,J)-B(2,N+1)*SIN(FLOAT(N*M)*C/D)
17    CONTINUE
      D=FLOAT(IYP)
      DO 20 J=1,IXP,1
      DO 18 I=1,IYP,1
      B(1,I)=0.
18    B(2,I)=0.
      DO 19 K=IYF1-1,IYF2-1,1
      DO 19 L=0,IYP-1,1
      B(1,K+1)=B(1,K+1)+(A(J,L+1)*COS(FLOAT(K*L)*C/D))/D
      B(2,K+1)=B(2,K+1)-(A(J,L+1)*SIN(FLOAT(K*L)*C/D))/D
19    CONTINUE
      DO 20 M=0,IYP-1,1
      A(J,M+1)=0.
      DO 20 N=IYF1-1,IYF2-1,1
      A(J,M+1)=A(J,M+1)+B(1,N+1)*COS(FLOAT(N*M)*C/D)
      A(J,M+1)=A(J,M+1)-B(2,N+1)*SIN(FLOAT(N*M)*C/D)
20    CONTINUE
39    CONTINUE
      IF(IM.EQ.0) GOTO 40
      WRITE(5,13)
      READ(5,14) SR
40    CONTINUE
      AMIN=A(1,1)
      AMAX=A(1,1)
      DO 21 I=1,IXP,1
      DO 21 J=1,IYP,1
      IF(A(I,J).GT.AMAX) AMAX=A(I,J)
21    IF(A(I,J).LT.AMIN) AMIN=A(I,J)
      IF(AMAX.EQ.AMIN) AMAX=AMAX+1.
      WRITE(5,22)
22    FORMAT(' DISPLACEMENT FIELD MAP:')
      DO 23 I=1,10,1
      DO 23 J=1,10,1
23    IT((I-1)*10+J)=J+47
      IT(101)=48
      WRITE(5,24) (IT(J),J=1,IXP+1,1)
24    FORMAT(1H ,101A1)
      DO 25 I=1,IXP,1
25    IT(I)=46
      KCR=49
```

```
      WRITE(5,26) KCR,(IT(J),J=1,IXP,1)
26    FORMAT(1H ,1A1,100A1)
      DO 33 I=IYP-1,2,-1
      KCR=KCR+1
      DO 31 M=2,IXP-1,1
31    IT(M)=46
      DO 32 J=2,IXP-1,1
      A1=(A(J,I)-AMIN)/(AMAX-AMIN)
      IF(A1.GT.SR) IT(J)=KA1
32    IF(A1.LE.SR) IT(J)=KA2
      WRITE(5,26) KCR,(IT(J),J=1,IXP,1)
      IF(KCR.EQ.57) KCR=47
      IM=0
      ITEST=IPEEK('177570)
      IF(ITEST.NE.0) IM=1
      IF(ITEST.EQ.1) GOTO 39
33    CONTINUE
      DO 34 I=1,IXP,1
34    IT(I)=46
      KCR=KCR+1
      WRITE(5,26) KCR,(IT(J),J=1,IXP,1)
      IF(ITEST.EQ.2) GOTO 39
      IM=0
      IF(ITEST.EQ.4) WRITE(5,11)
      IF(ITEST.EQ.4) READ(5,12) IXF1,IXF2,IYF1,IYF2
      IF(ITEST.EQ.4) GOTO 9
      IF(ITEST.EQ.8) GOTO 41
      IF(ITEST.EQ.16) WRITE(5,42)
42    FORMAT(' HIGH, LOW ASCII CODES-2I2')
      IF(ITEST.EQ.16) READ(5,43) KA1,KA2
43    FORMAT(2I2)
      IF(ITEST.EQ.16) GOTO 40
      IF(ITEST.EQ.64) GOTO 35
      IF(ITEST.NE.32) GOTO 10
      IBX=1
      IBY=IYP
      IXS=IABS(IXS)
      IYS=IABS(IYS)
44    WRITE(5,45)
45    FORMAT(' X,Y INPUT POSITION-2I3')
      READ(5,3) IZX,IZY
      I1=(IZX-IBX)*IXS
      I2=-(IZY-IBY)*IYS
      IF(I1.NE.0) CALL XADV(I1,5)
      IF(I2.NE.0) CALL YADV(I2,5)
      IBX=IZX
      IBY=IZY
      IF(IZX.NE.1.OR.IZY.NE.IYP) GOTO 44
      GOTO 10
35    CONTINUE
      STOP
      END
      SUBROUTINE XADV(IS,IR)
      X=0.
      IF(IS.GT.0) GOTO 3
      IP=IABS(IS)
      DO 2 I=1,IP,1
      CALL IPOKE('167772,'100000)
      DO 7 K=1,IR,1
7     Y=SIN(X)
      CALL IPOKE('167772,'000000)
      DO 1 J=1,IR,1
1     Y=SIN(X)
2     CONTINUE
      GOTO 6
3     CONTINUE
```

```
      DO 5 II=1,IS,1
      CALL IPOKE('167772,'040000)
      DO 8 KK=1,IR,1
8     Y=SIN(X)
      CALL IPOKE('167772,'000000)
      DO 4 JJ=1,IR,1
4     Y=SIN(X)
5     CONTINUE
6     CONTINUE
      RETURN
      END
      SUBROUTINE YADV(IS,IR)
      X=0.
      IF(IS.GT.0) GOTO 3
      IP=IABS(IS)
      DO 2 I=1,IP,1
      CALL IPOKE('167772,'020000)
      DO 7 K=1,IR,1
7     Y=SIN(X)
      CALL IPOKE('167772,'000000)
      DO 1 J=1,IR,1
1     Y=SIN(X)
2     CONTINUE
      GOTO 6
3     CONTINUE
      DO 5 II=1,IS,1
      CALL IPOKE('167772,'010000)
      DO 8 KK=1,IR,1
8     Y=SIN(X)
      CALL IPOKE('167772,'000000)
      DO 4 JJ=1,IR,1
4     Y=SIN(X)
5     CONTINUE
6     CONTINUE
      RETURN
      END
*
```

LIST OF SYMBOLS

Symbol	Definition
Cn	Discrete Fourier transform frequency spectral components
2d	Spacing between n = 1/2 fringe orders
dv	Vertical vectoral component of d
dH	Horizontal vectoral component of d
f	Distance from interferogram to analyzer screen
I(K)	Digitized intensity data
I'(K)	Filtered intensity data
J	Imaginary number
N	Total number of data samples
n	Fringe order of contour
S	Film scale factor
$U\theta$	Absolute displacement along θ axis
Uv	Absolute displacement along vertical axis
U_H	Absolute displacement along horizontal axis
α	Lower harmonic level of DFT filter

β	Upper harmonic level for DFT filter
λ	Wavelength of laser light source
θ	Angle
ν	Optical geometrical constant
χ	Photodetector offset distance

DISTRIBUTION

	No. of Copies
Defense Documentation Center Cameron Station Alexandria, Virginia 22314	12
Defense Metals Information Center Battelle Memorial Institute 505 King Avenue Columbus, Ohio 43201	1
Commander US Army Foreign Science and Technology Center ATTN: DRXST-SD3 220 Seventh Street, NE. Charlottesville, Virginia 22901	1
Office of Chief of Research and Development Department of the Army ATTN: DARD-ARS-P Washington, DC 20301	1
Commander US Army Electronics Command ATTN: DRSEL-PA-P -CT-DT -PP, Mr. Sulkolove Fort Monmouth, New Jersey 07703	1 1 1
Commander US Army Natick Laboratories Kansas Street ATTN: STSNLT-EQR Natick, Massachusetts 01760	1
Commander US Army Mobility Equipment Research and Development Center Fort Belvoir, Virginia 22060	1

DISTRIBUTION

	No. of Copies
Director USA Mobility Equipment Research and Development Center Coating and Chemical Laboratory ATTN: STSFB-CL Aberdeen Proving Ground, Maryland 21005	1
Commander Edgewood Arsenal ATTN: SAREA-TS-A Aberdeen Proving Ground, Maryland 21010	1
Commander Picatinny Arsenal ATTN: SARPA-TS-S, Mr. M. Costello Dover, New Jersey 07801	1
Commander Rock Island Arsenal Research and Development ATTN: 9320 Rock Island, Illinois 61201	1
Commander Watervliet Arsenal Watervliet, New York 12189	1
Commander US Army Aviation Systems Command ATTN: DRSAV-EE -MT, Mr. Vollmer St. Louis, Missouri 63166	1 1
Commander US Army Aeronautical Depot Maintenance Center (Mail Stop) Corpus Christi, Texas 78403	1
Commander UA Army Test and Evaluation Command ATTN: DRSTE-RA Aberdeen Proving Ground, Maryland 21005	1

DISTRIBUTION

	No. of Copies
Commander ATTN: STEAP-MT Aberdeen Proving Ground, Maryland 21005	1
Chief Bureau of Naval Weapons Department of the Navy Washington, DC 20390	1
Chief Bureau of Ships Department of the Navy Washington, DC 20315	1
Naval Research Laboratory ATTN: Dr. M.M. Krafft Code 8430 Washington, DC 20375	1
Commander Wright Air Development Division ATTN: ASRC Wright-Patterson AFB, Ohio 45433	1
Director Air Force Materiel Laboratory ATTN: AFML-DO-Library Wright-Patterson AFB, Ohio 45433	1
Director Army Materials and Mechanics Research Center ATTN: DRXMR-PL -MT, Mr. Farrow Watertown, Massachusetts 02172	1 1
Commander White Sands Missile Range ATTN: STEWS-AD-L White Sands Missile Range, New Mexico 88002	1
Deputy Commander US Army Nuclear Agency ATTN: MONA-ZB Fort Bliss, Texas 79916	1

DISTRIBUTION

	No. of Copies
Jet Propulsion Laboratory California Institute of Technology ATTN: Library/Acquisitions 111-113 4800 Oak Grove Drive Pasadena, California 91103	1
Sandia Laboratories ATTN: Library P.O. Box 969 Livermore, California 94550	1
Commander US Army Air Defense School ATTN: ATSA-CD-MM Fort Bliss, Texas 79916	1
Technical Library Naval Ordnance Station Indian Head, Maryland 20640	1
Commander US Army Materiel Development and Readiness Command ATTN: DRCMT Washington, DC 20315	1
Headquarters SAC/NRI (Stinfo Library) Offutt Air Force Base, Nebraska 68113	1
Commander Rock Island Arsenal ATTN: SARRI-KLPL-Technical Library Rock Island, Illinois 61201	1
Commander (Code 233) Naval Weapons Center ATTN: Library Division China Lake, California 93555	1
Department of the Army US Army Research Office ATTN: Information Processing Office P.O. Box 12211 Research Triangle Park, North Carolina 27709	1

DISTRIBUTION

	No. of Copies
ADTC (DLDSL) Eglin Air Force Base, Florida 32542	1
University of California Los Alamos Scientific Laboratory ATTN: Reports Library P.O. Box 1663 Los Alamos, New Mexico 87545	1
Commander US Army Materiel Development and Readiness Command ATTN: DRCRD	1
DRCDL 5001 Eisenhower Avenue Alexandria, Virginia 22333	1
Director Defense Advanced Research Projects Agency 1400 Wilson Boulevard Arlington, Virginia 22209	1
DRSMI-LP, Mr. Voigt	1
DRSMI-X	1
-T, Dr. Kobler	1
-TL, Mr. Lewis	1
-TLA, Mr. Pettey	1
-TLA, Dr. Mullinix	1
Mr. Schaeffel	50
-EA	2
-EAA	2
-EAS	1
-EAM	1
-EAP	1
-EAB	1
-EAT	3
-ICBB	1
-TBD	3
-TI (Record Set)	1
(Reference Copy)	1

DISTRIBUTION (Concluded)

	No. of Copies
Commander US Army Research Office ATTN: DRXRO-PW, Dr. R. Lontz P.O. Box 12211 Research Triangle Park, North Carolina 27709	2
US Army Research and Standardization Group (Europe) ATTN: DRXSN-E-RX, Dr. Alfred K. Nodoluha Box 65 FPO New York 09510	2
Headquarters Department of the Army Office of the DCS for Research Development and Acquisition Room 3A474, The Pentagon ATTN: DAMA-ARZ Washington, DC 20310	2
US Army Materiel Systems Analysis Activity ATTN: DRXSY-MP Aberdeen Proving Ground, Maryland 21005	1
IIT Research Institute ATTN: GACIAC 10 West 35th Street Chicago, Illinois 60616	1